32nd URSI GASS, Montreal, 19-26 August 2017

Recent Advances in VLBI Astrometry

Richard Dodson* (1) and María Rioja (1,2,3)
(1) ICRAR, University of Western Australia, Perth Australia
(2) CSIRO Astronomy and Space Science, 26 Dick Perry Avenue, Kensington WA 6151, Australia
(3) Observatorio Astronómico Nacional (IGN), Alfonso XII, 3 y 5, 28014 Madrid, Spain

Abstract

We provide a summary of recent work we have performed to extend phase referencing to hither-to unreachable regimes. These include very high frequencies (mm and sub-mm) where the short coherence times have prevented source switching; low frequencies, where direction dependent effects prevent source phase transfer; and decomposing the atmosphere into the Ionospheric and Tropospheric components and then correcting for these piece-wise.

Results from these three approaches, Source Frequency Phase Referencing, Multi-View Phase Referencing and Multi-Frequency Phase Referencing, are presented in the context of the contribution of the atmosphere, which is to be corrected.

1. Introduction

Very Long Baseline Interferometry (VLBI) can result in the highest angular resolutions achieved in astronomy and has a unique access to emission regions that are inaccessible with any other approach. Therefore it holds the potential to increase our understanding of the physical processes in e.g. Active Galactic Nuclei (AGN), in the vicinity of super-massive Black Holes, and for studies of molecular transitions at high frequencies. One of the most powerful applications of VLBI is in the measurement of high precision relative astrometric angles between sources. Because of the fact that the reference source are (usually) Quasars (QSOs) at high red shifts this has allowed measurement of parallaxes without biases to ~10μas, sufficient to measure distances across our Galaxy. An accurate (i.e. astrometric) registration of images (be they total intensity, polarised emission, spectral line or others) obtained at different frequencies is crucial to form a meaningful interpretation based on multi-frequency comparisons, in a similar manner as is required between epochs for multi-epoch temporal studies. Bona fide astrometry can be achieved with a suitable calibration strategy that removes the contributions of the medium through which the signal propagates, while retaining the intrinsic astrometric signature of the source in the phase observable. If so, the astrometric accuracy is ultimately limited by the uncertainty in the precise phase observable and reaches the thermal limit of the instrument ($\sigma_{pos} \sim \theta_B/SNR$, where σ_{pos} is the accuracy, θ_B is the synthesised beam and SNR is the Signal to Noise) which leads to μ-as astrometry. Phase referencing does this, by interleaving observations of a second source.

Nevertheless the applications of astrometric-VLBI are not widespread outside of the centimetre wavelengths; say 5–22GHz. The observations become progressively more challenging away from these frequencies. For the higher frequencies the system temperatures increase and the atmospheric coherence times fall. For the lower frequencies the recording bandwidth are smaller (as the central frequency approaches zero) and the atmospheric solutions are wildly different for different lines of sight. We have been developing a number of methods that correct for the atmospheric contamination at both the high and low frequency range.

We take as our starting point for consideration of potential approaches to astrometry the formulae in [1], which provide a rough guide for the magnitude of contaminating signals in phase-referencing experiments. Table 1 shows that the tropospheric phases scale with frequency, and the ionosphere scales with wavelength. That is the tropospheric phase errors are true delays and therefore non-dispersive, whereas the ionospheric errors are dispersive delay.

	Static	Dynamic
Tropo-sphere	$14\frac{\nu}{8}\frac{\Delta l}{3}$	$5\,Cw\frac{\nu}{8}\frac{\sec Z}{\sec(45)}^{1/2}$
Phase error (°)	$[(\frac{\Delta\theta}{2})\frac{\cos(45)}{\cos(Z)}\frac{\tan(Z)}{\tan(45)}]$	$[\frac{T_{swt}}{60}+(0.16\frac{\Delta\theta}{2}\frac{\sec Z}{\sec(45)})]^{5/6}$
Iono-sphere	$14.5\,(\frac{\nu}{8})^{-1}\frac{\Delta I}{6}$	$2.5\,(\frac{\nu}{8})^{-1}\frac{\sec Z}{\sec(43)}^{1/2}$
Phase error (°)	$[(\frac{\Delta\theta}{2})\frac{\cos(41)}{\cos(Z)}\frac{\tan(Z)}{\tan(41)}]$	$[(\frac{\Delta\theta}{2}\frac{\sec Z}{\sec(43)})+(0.21\frac{T_{swt}}{60})]^{5/6}$

Table 1 Formulae from [1] for the typical atmospheric phase errors on a VLBI baseline, at 8GHz. ν is the frequency in GHz, C_w is the atmospheric condition (1, 2 and 4 being good, typical and poor). T_{swt} is the source switching duty cycle in sec, Δl is the residual zenith path length in cm, ΔI is the residual TEC, Δθ is the angular separation in degrees, Z is the Zenith angle from the ground and from the ionospheric plane, for troposphere and ionosphere respectively.

The contributions are about equal at ~8GHz, when Δl is 3cm and ΔTEC of 6TECU. We use this boundary to define the division between 'high' and 'low' frequency domains. Note that the static terms are more significant than the dynamic terms; also the latter affect only the precision, whereas the former affect the accuracy. The dynamic tropospheric errors are dominated by the switching time, the static troposphere scales with the combination of angular separation and the residual atmospheric path length errors. For the ionospheric phases the dynamic errors are dominated by the angular separation and the static errors scale with the combination of angular separation and the residual total electron content of the atmosphere.

Using these formulae one can easily find the most important experimental consideration for any particular experiment. For example, geodetic blocks, used extensively for the BeSSeL project to reduce the residual path length Δl from 3cm to 1cm, can reduce the contribution of the static tropospheric component, which dominates at 22GHz. VERA on the other hand reduces the dynamic tropospheric component by simultaneously observing the calibrator and the target, setting T_{swt} to zero. Alternatively in-beam astrometry minimises Δθ, reducing contributions from static troposphere and the ionosphere. This however only works well where the primary beam is large, i.e. around L-band. None of these methods are reducing the error contributions to zero, unlike the methods below.

2. Source Frequency Phase Referencing

Source/Frequency Phase Referencing (SFPR) analysis consists of two calibration steps and are fully discussed in [2,3,4,5]. In a first step, the observations at the higher frequency bands are calibrated using the simultaneous observations at a lower frequency band, for each source. This dual frequency calibration step eliminates the common non-dispersive residual errors (e.g. tropospheric propagation effects and inaccurate coordinates, i.e. correcting Δl to zero) in the complex visibility output of the correlator, providing increased signal coherence at the higher frequency. The second step of the calibration removes the remaining dispersive residual errors (i.e. instrumental and ionospheric propagation effects) using the interleaving observations of another source. This two-step calibration retains the astrometric signature of any source position shifts between the two frequencies. The Fourier transformation of this dataset is the SFPR map, which conveys a bona fide astrometric measurement of the relative separation or shift between the positions of the reference points in the images at the two frequencies, for the two sources.

Figure 1 shows the spectral index for astrometrically registered observation made at the Koren VLBI Network (KVN), with the 22-GHz image aligned with the 43-, 86- and 130-GHz images. See [5;6] for observational details and discussions.

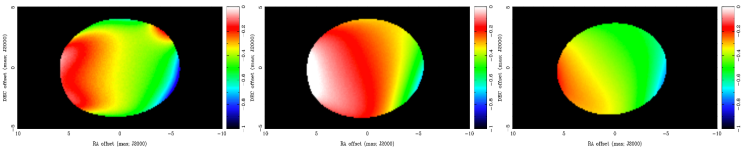

Figure 1. Spectral indices for the SFPR observations discussed in [16,15], for 1807+698 between 22- and 43-, 86- and 130-GHz.

3. Multi-Frequency Phase Referencing

The SFPR method has been demonstrated with frequencies as high as 130GHz (2mm) [5]. However SFPR requires a second calibrator source with-in about 10^o of the target. The density of calibrators at 86GHz, or even at 43GHz, is not sufficient to guarantee that a suitable source will be within this range. Indeed, this was the case for observations of BL-Lac [7].

Therefore we attempted to achieve phase referencing in a similar fashion to SFPR, but without the second source. Our approach is to calibrate all frequencies against a well-known source with precise astrometric position, then solve for the residual delays for the target, across a wide frequency span. This allows us to measure (and remove) the residual TEC (i.e. setting ΔI to zero) in the target direction, which is used to produce an ionosphere-free dataset for all frequencies. Therefore the second calibration step in SFPR is no longer required. This method we dubbed Multi-Frequency Phase Referencing (MFPR), as now our calibration scheme allows relative astrometry between the (mm) frequency bands corrected by observations at multiple (cm) frequencies of the target.

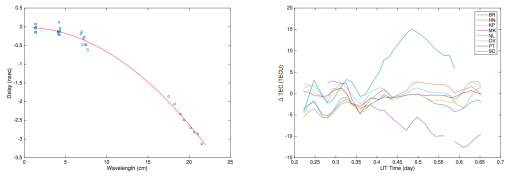

Figure 2. *Left*) A typical delay $\tau(\nu)$ for one particular antenna (BR) and 2 minute scan (UT 05:56), as a function of wavelength. It shows the curvature (following ν^{-2}) that directly measures the ΔTEC residual (-4.4 TECU, solid line). *Right*) The ΔTEC residuals for all antennas across the duration of the experiment. The values for most antennas range between ±5 TECU. The antennas MK and SC show the largest deviations. Errors are typically 0.1 TECU.

For the ionospheric correction blocks we use the delay (only) from each IF to measure the Total Electron Content (TEC) contribution on the line of sight towards BL-Lac, as a function of time, as shown in Figure 2. This is a measurement of the residual ionospheric contribution, after correction with the GPS data and the subtraction of the TEC in the direction of the prime calibrator, at the time of that scan. We fitted a linear slope in ν^{-2} to the semi-simultaneous delay measurements (i.e. such that $\tau(\nu)=\tau_{trop}+\tau_{iono}\nu^{-2}$) and calculate the residual TEC contribution as a function of time, for that line of sight. Here $\tau(\nu)$ are the measured delays as a function of frequency for one block of ionospheric calibration observations, τ_{trop} is the non-dispersive delay (from both clock and tropospheric contributions), τ_{iono} is the ionospheric delay (at 1 GHz). The derived ΔTEC is then used to calculate the ionospheric contribution for each IF, at each time interval. Finally we solved for the (ionosphere-free) delay, rate and phase on the (ionosphere-corrected) 22 GHz data and applied these solutions, suitably scaled by the frequency ratio, to the ionosphere-corrected 43 and 86 GHz data to obtain data free of any atmospheric contamination, for astrometric imaging. See [7] for details.

4. Multi-View Phase Referencing

To increase the capability for high precision astrometric measurements at low radio frequencies (<8 GHz) we have developed another new calibration strategy. Observations at low frequencies are dominated by distinct direction dependent ionospheric propagation errors, which place a very tight limit on the angular separation $\Delta\theta$ of a suitable phase referencing calibrator.

The MultiView technique (MV) uses observations of multiple distant (~degrees) calibrators and 2-D interpolation of the solutions to the line of sight of the target. Therefore this is equivalent to observing with a $\Delta\theta$ of zero. The first comparative study of the astrometric accuracy between MultiView and phase-referencing (PR) techniques is to be found in [8]. It is a development of the "cluster–cluster" VLBI technique [9;10].

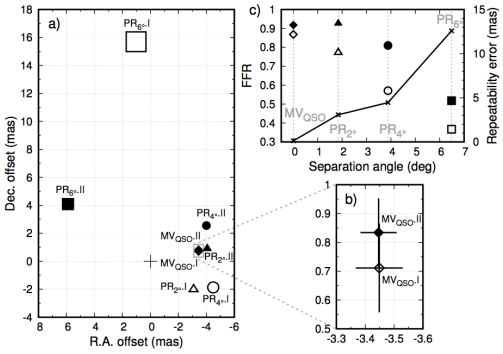

Figure 3. a) Astrometric offsets in the angular separations measured with MV and PR (see [8] for details) for two epochs. The size of the symbols corresponds to the error. The labels describe the analysis id. and epoch. b) Zoom-in on MV astrometric solutions. Both epochs agree within errors. c) Solid line shows the repeatability astrometric errors vs the angular separation between target and calibrator for PR, and at zero separation for MV. Symbols show the Fractional Flux Recovery vs angular separation for MV (diamond), PR_{2^o} (triangle), PR_{4^o} (circle), and PR_{6^o} (square) analyses, for epoch I (empty) and II (filled).

The MV calibration strategy corrects for the direction dependent nature of the ionospheric

phase errors by using simultaneous or near-simultaneous observations of multiple calibrators around the target. Then we use a 2-D interpolation of the antenna phases (whilst solving for untracked 2π phase ambiguities), estimated along the directions of all calibrators, to provide corrections along the line of sight of the target observations. This is realized by a weighted linear combination of the complex antenna gains, representing the relative source distribution in the sky. This is equivalent to the treatment of the propagation medium as a wedge-like spatial structure, up to several degrees in size, above each antenna [8]. The temporal structure of the propagation medium effects is best calibrated using simultaneous observations of the calibrators and the target sources (i.e. T_{swt} of zero). However when this observing configuration is not possible one can use alternating observations of the sources, as long as the duty cycle is less than the atmospheric coherence time. The formulae is Table 1 allow one to calculate this for the Ionosphere; these timescales are typically many minutes. We have tested this approach on 1.6GHz OH and 6.7 CH_3OH masers. Figure 3 is taken from [8] and compares PR and MV 1.6-GHz calibration of a in-beam QSO near the OH maser. MultiView calibration provides an order of magnitude improvement in astrometry with respect to conventional phase referencing, achieving ~100μas astrometry errors in a single epoch of observations, effectively reaching the thermal noise limit. Similar results have been obtained with a BeSSeL VLBA observation of a 6.7 CH_3OH maser, which had four calibration sources. MV achieved the same accuracy, albeit with slightly worse precision, despite the experimental design not being optimised for MV. Therefore MV seems to achieve a superior mitigation of atmospheric errors that results in increased precision astrometry, along with wide applicability by relaxing the constraints on the angular separation up to few degrees, and does not require alignment of sources. The scope of application is for the low frequency regime where the performance of PR is degraded due to the spatial structure of the ionospheric dominant errors.

5. Conclusions

We have discussed new methods that correct for atmospheric contributions to astrometry errors.

Source Frequency Phase Referencing is now well demonstrated and is in use for a multitude of different projects, which are providing bona-fide alignment of AGNs [4;5], SiO masers [11], H_2O and SiO masers [12]. It is mainly used on the KVN, as the simultaneous multiband receivers simplifies the analysis. However it has been performed on the VLBA [2;3;13] and global simultaneous multiband receivers are being added (currently VERA, ATCA and Yebes).

Multi-Frequency Phase Referencing has only been demonstrated on one source [7] but many more observations are being analysed. The foundations seem solid and the fast frequency switching of the VLBA makes the implementation straight forward.

MultiView will achieve its full potential with the enhanced sensitivity and multibeam capabilities of SKA and the pathfinders, which will enable simultaneous observations of the target and calibrators. Nevertheless our demonstration indicates that both the 10μas goal of astrometry at 1.6GHz using VLBI with SKA, and high precision astrometry at low-frequencies are possible with the VLBA, are feasible using the MultiView technique.

6. References

[1] Y. Asaki, etal, "Verification of the Effectiveness of VSOP-2 Phase Referencing with ARIS," PASJ, 59, 397, 2007.

[2] R. Dodson and M. J. Rioja, "VLBA Scientific Memorandum #31: Astrometric calibration of mm-VLBI using "Source/Frequency Phase Referenced" observations, tech. rep., NRAO, Oct. 2009.

[3] M.Rioja and R.Dodson, "High-precision Astrometric mm-VLBI Using a New Method for Atmospheric Calibration," AJ, 141, 114. 2011

[4] M. J. Rioja, etal, "Verification of the Astrometric Performance of the Korean VLBI Network, Using Comparative SFPR Studies with the VLBA at 14/7 mm," AJ. 148, 84, 2014.

[5] M. J. Rioja, etal, "Simultaneous Multi-Frequency Observations for mm-VLBI: KVN Astrometry up to 130GHz," AJ, 150, 202, 2015.

[6] M. J. Rioja, etal., "The Power of Simultaneous Multi-Frequency Observations for mm-VLBI and Astrometry," Galaxies, 5, 9 2017.

[7] R. Dodson, etal, "High-precision Astrometric Millimeter Very Long Baseline Interferometry Using a New Method for Multi-frequency Calibration," ApJ, 834,177,.2017

[8] M. J. Rioja, etal, "MultiView High Precision VLBI Astrometry at Low Frequencies", arXiv:1612.02554, Dec. 2016.

[9] M. J. Rioja, etal, "VLBI observations in Cluster-Cluster mode at 1.6 GHz," in Proceedings of the 6th EVN Symposium (E. Ros, R. W. Porcas, A. P. Lobanov, and J. A. Zensus, eds.), p. 57, June 2002.

[10] M. Rioja, etal, "Revisited "Cluster-Cluster" VLBI with multi-beam low frequency radio interferometers," in 8th Int. e-VLBI,14, 2009.

[11] Cho, "4 band SiO maser KVN observations" ApJ, in prep., 2017.

[12] R. Dodson, etal, "Astrometrically Registered Observations of H_2O and SiO Masers," AJ, 148, 97, 2014.

[13] I. Marti-Vidal, etal, "Absolute kinematics of radio-source components in the complete S5 polar cap sample. IV," A&A, 596, 27